



**HAL**  
open science

## Combining two repurposed drugs as a promising approach for Alzheimer's disease therapy

Ilya Chumakov, Serguei Nabirotkin, Nathalie Cholet, Aude Milet, Aurélie Boucard, Damien Toulorge, Yannick Pereira, Esther Graudens, Sory Traore, Julie Fouquier, et al.

### ► To cite this version:

Ilya Chumakov, Serguei Nabirotkin, Nathalie Cholet, Aude Milet, Aurélie Boucard, et al.. Combining two repurposed drugs as a promising approach for Alzheimer's disease therapy. *Scientific Reports*, 2015, 5 (1), 10.1038/srep07608 . hal-01922611

**HAL Id: hal-01922611**

**<https://hal.science/hal-01922611>**

Submitted on 27 May 2021

**HAL** is a multi-disciplinary open access archive for the deposit and dissemination of scientific research documents, whether they are published or not. The documents may come from teaching and research institutions in France or abroad, or from public or private research centers.

L'archive ouverte pluridisciplinaire **HAL**, est destinée au dépôt et à la diffusion de documents scientifiques de niveau recherche, publiés ou non, émanant des établissements d'enseignement et de recherche français ou étrangers, des laboratoires publics ou privés.



Distributed under a Creative Commons Attribution 4.0 International License



## OPEN

## Combining two repurposed drugs as a promising approach for Alzheimer's disease therapy

## SUBJECT AREAS:

ALZHEIMER'S DISEASE

CLINICAL PHARMACOLOGY

Received  
20 October 2014Accepted  
19 November 2014Published  
8 January 2015Correspondence and  
requests for materials  
should be addressed to  
D.C. (dcohen@  
pharnext.com)

Ilya Chumakov<sup>1</sup>, Serguei Nabirotkhin<sup>1</sup>, Nathalie Cholet<sup>1</sup>, Aude Milet<sup>1</sup>, Aurélie Boucard<sup>1</sup>, Damien Toulorge<sup>1</sup>, Yannick Pereira<sup>1</sup>, Esther Graudens<sup>1</sup>, Sory Traoré<sup>1</sup>, Julie Fouquier<sup>1</sup>, Mickael Guedj<sup>1</sup>, Emmanuel Vial<sup>1</sup>, Noëlle Callizot<sup>2</sup>, Rémy Steinschneider<sup>3</sup>, Tanguy Maurice<sup>4,5</sup>, Viviane Bertrand<sup>1</sup>, Catherine Scart-Grès<sup>1</sup>, Rodolphe Hajji<sup>1</sup> & Daniel Cohen<sup>1</sup>

<sup>1</sup>Pharnext, 11 rue des Peupliers, 92130 Issy-Les-Moulineaux, France, <sup>2</sup>Neuro/Sys, 410 CD 60, 13120 Gardanne, France, <sup>3</sup>Neuronexperts, 51 bd Pierre Dramard, 13916 Marseille, France, <sup>4</sup>Université de Montpellier 2, 34095 Montpellier, France; Inserm, U710, 34095 Montpellier, France; EPHE, 75017 Paris, France, <sup>5</sup>Amylgen, 2196 bd de la Lironde, 34980 Montferrier-sur-Lez, France.

Alzheimer disease (AD) represents a major medical problem where mono-therapeutic interventions demonstrated only a limited efficacy so far. We explored the possibility of developing a combinational therapy that might prevent the degradation of neuronal and endothelial structures in this disease. We argued that the distorted balance between excitatory (glutamate) and inhibitory (GABA/glycine) systems constitutes a therapeutic target for such intervention. We found that a combination of two approved drugs – acamprosate and baclofen – synergistically protected neurons and endothelial structures *in vitro* against amyloid-beta (A $\beta$ ) oligomers. The neuroprotective effects of these drugs were mediated by modulation of targets in GABA/glycinergic and glutamatergic pathways. *In vivo*, the combination alleviated cognitive deficits in the acute A $\beta_{25-35}$  peptide injection model and in the mouse mutant APP transgenic model. Several patterns altered in AD were also synergistically normalised. Our results open up the possibility for a promising therapeutic approach for AD by combining repurposed drugs.

Alzheimer's disease (AD) is a lethal neurodegenerative disorder of older persons, affecting nearly 40 million patients worldwide. Clinically it is manifested by rapid progressive deterioration leading to the loss of independence. Mental capacities involving memory, language and everyday functioning are affected and this loss is often accompanied by psychosis. With the aging of world population and emerging of new effective treatments for other mortal diseases the importance of AD as an economic burden and limiting factor of life duration is progressively becoming more and more important. To date, all treatment options are marginally effective<sup>1</sup> and preserve cognitive function only temporarily<sup>2</sup>. In AD, brain regions involved in cognitive functions show a series of abnormalities including progressive loss of neurons and synapses and signs of neuroinflammation, accompanied by neuronal degeneration<sup>3</sup>. In addition, the brain of AD patients often shows cerebrovascular defects such as abnormal permeability of the blood-brain barrier (BBB)<sup>4</sup>. Significant comorbidity between AD and cerebrovascular deregulation suggests that these defects are important features of AD<sup>5</sup>. Abnormal metabolism of amyloid precursor protein (APP) results in production of cytotoxic A $\beta$  peptide oligomers and formation of extracellular amyloid plaques, histopathological hallmarks of AD. The attempts of therapeutic intervention at the level of processing and turnover of these peptides have failed so far<sup>6</sup>. The etiological factors leading to AD are not fully understood. They might act synergistically with amplifying feed-back loops<sup>7</sup> implicating these peptides and other toxic factors, making the disease state resistant to mono-therapeutic interventions.

To affect the different elements that appear to contribute to this complex disorder, we are proposing here a new combinational approach. The systematic analysis of available genetic and functional data in the literature has drawn our particular attention to the disturbance in the balance between glutamate, GABA, and glycine systems for the development of pathological features prominent in AD that could play a role in degeneration of brain structures. Glutamate system in the brain is not only important for signal transmission and plasticity but also for the regulation of survival or induction of apoptosis of brain cells. This system is counter-balanced by inhibitory GABA and glycine signalling with normal brain functions assured by the subtle equilibrium between these inhibitory and excitatory (E/I) activities.

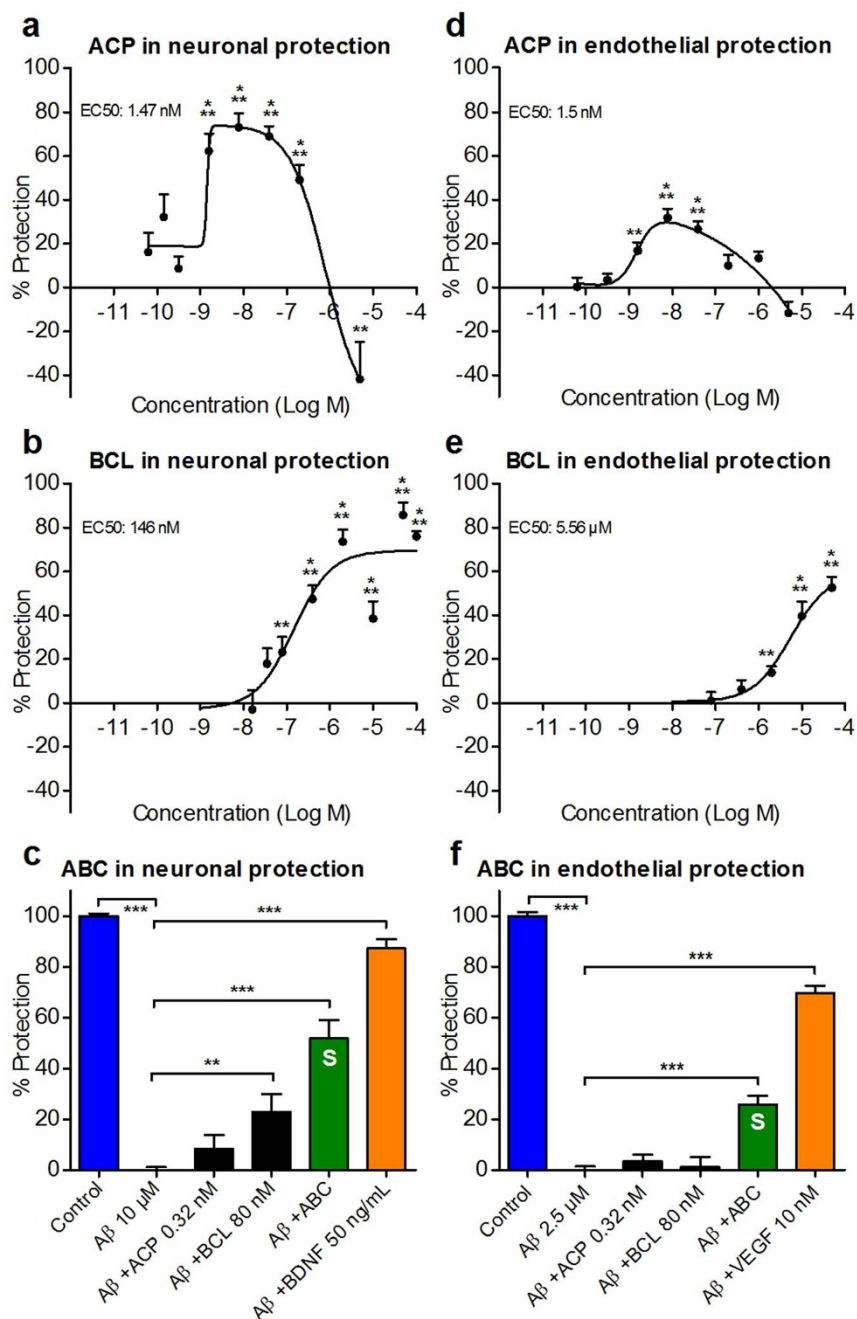


**Figure 1** | Combination of ACP and BCL acts synergistically to protect neurons and microvascular HBMEC tubules from the toxicity of  $A\beta_{1-42}$  oligomers. Normalised data for the difference between  $A\beta_{1-42}$  oligomer-treated and untreated cultures are presented. The dose-response curve of ACP in primary neurons and HBMEC (a,d) showed a bell-shaped protective aspect in both assays, while that of BCL was sigmoid (b,e). At sub-active concentrations of individual drugs, ABC was active with a synergistic effect on neuronal (c) ( $n = 7$ ) and HBMEC tubular (f) ( $n = 3$ ) protection. BDNF (c) and VEGF (f) were used as controls. All values are mean  $\pm$  s.e.m. \*\* $P < 0.01$ , \*\*\* $P < 0.001$  versus  $A\beta$ ; ANOVA with Dunnett's test. S: Synergy.

Deregulation of glutamate excitatory neuronal signalling has been proposed as a neurophysiological mechanism responsible for cognitive impairment in AD<sup>8</sup>. While GABAergic neurons are considered to be relatively preserved in AD patients<sup>9</sup>, a recent study has demonstrated a profound remodelling of molecular components of GABAergic neurotransmission<sup>10</sup> with complex changes in the relative concentrations of its different molecular constituents, which by themselves could compromise the overall balance of E/I signalling.

We argued that the chronic presence of toxic  $A\beta$  oligomers could modify this balance, thereby impairing cognitive functions and enhancing the pro-apoptotic activity both in neuronal and endothelial cells. Thus, we have selected several candidate drugs, each poten-

tially acting on multiple targets in these pathways. Since our ultimate goal has been to progress rapidly toward the AD treatment development, we focused on drugs that met two principal criteria: 1) used for a long time to treat other disorders<sup>11</sup>, and 2) having a good safety profile.

The first chosen drug is acamprostate calcium (ACP), an anti-craving agent that is thought to influence glutamatergic transmission and to affect the E/I balance distorted in ethanol addiction. ACP is a safe drug being used at exceptionally high doses. ACP decreases glutamate levels induced in human brain during ethanol withdrawal and reverses the resulting hyperexcitability<sup>12</sup>. Glutamate receptors are important both for the balance between cell death and survival<sup>13</sup>.

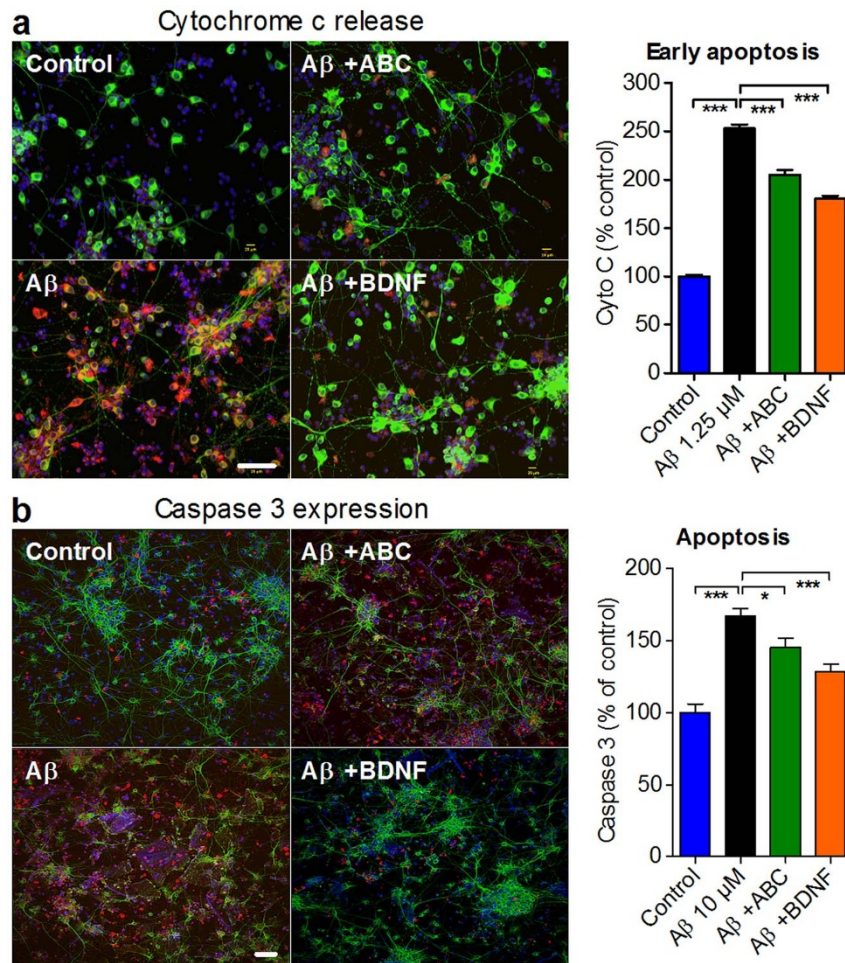


**Figure 2** | ABC action to reduce  $A\beta_{1-42}$ -induced cell death is mediated by preventing apoptosis. Positive effect of ABC on apoptosis assessed by Cyto c (a) and caspase 3 (b) staining. Neurons with Cyto c or caspase 3 (in red) overlapping with MAP2 (in green) were counted and results were expressed as percentage of untreated control. Scale bars: 60  $\mu$ m. Values are mean  $\pm$  s.e.m. \* $P < 0.05$ , \*\*\* $P < 0.001$  versus A $\beta$ ; ANOVA with Dunnett's test. ABC was composed of 0.32 nM ACP and 80 nM BCL. BDNF was used as positive control (50 ng mL<sup>-1</sup>). MAP2: Microtubule-associated protein 2. Blue: Hoechst.

Their function is substantially modified in AD<sup>14</sup>. Possible targets for ACP include the iono/metabotropic glutamate receptors<sup>15</sup> but also inhibitory glycine gated ion channels<sup>16</sup>.

Furthermore, we thought that to be effective and to resist the possible feedback changes during chronic treatment, we should use a drug combination that acts also on the brain major inhibitory system: GABA. We therefore selected a second drug, (RS)-baclofen (BCL), used for the treatment of spasticity for several decades and which activates inhibitory metabotropic GABA<sub>B</sub> receptors. BCL has rather favourable safety profile even when used at high doses and is the only agonist of GABA<sub>B</sub> receptors that is authorised for human use. It should also be noticed that glutamate, GABA and glycine receptors targeted by ACP and BCL are also important for the function of the endothelial BBB<sup>17-19</sup>.

At this stage we decided to test ACP or BCL alone and in combination (ABC) in a battery of cellular and animal paradigms. No satisfactory model exists for AD<sup>20</sup>, but we concentrated our efforts on multiple observational endpoints that are mimicked in these models to provide a substantial rationale for the future testing in AD patients.

## Results

**ABC synergistically protects against A $\beta$  toxicity in AD *in vitro* models.** To test the protective potential of ABC against the effects of toxic soluble oligomeric A $\beta_{1-42}$  peptides, we used two models: a primary culture of rat cortical neurons<sup>21</sup>, and a primary culture of human brain-derived microvascular endothelial cells (HBMEC) that form a tubular network in matrigel<sup>22</sup>. We used the same batch of

A $\beta_{1-42}$  peptides described by us previously<sup>21</sup>. This batch, extensively studied by several techniques contained low and high molecular weight A $\beta_{1-42}$  oligomers as assessed by Western blot analyses using the 6E10 antibody. We verified that only preparations containing A $\beta_{1-42}$  oligomers were able to induce toxicity in neuronal cultures, while initial peptide preparation that did not contain oligomers was not toxic<sup>21</sup>, excluding a nonspecific effect of contaminating agents. This allowed us to use non-treated cells as controls without the need for using scrambled peptides as negative controls. At low doses, ACP (Fig. 1a,d) and BCL (Fig. 1b,e) alone protected neurons as well as the microvascular network against A $\beta_{1-42}$  toxicity (Supplementary Table 1). To test for possible additive or synergistic interactions between the two drugs, sub-active doses (doses only marginally active in both assays) were used (Supplementary Fig. 1a,b). We found significantly greater neuronal and vascular cell protection from A $\beta_{1-42}$  toxicity with ABC compared to the effect of each drug individually (Fig. 1c,f). This positive interaction between ACP and BCL was confirmed by calculation of Combination Indexes and isobolograms (Supplementary Fig. 1c) for a range of ABC doses and ratios (Supplementary Fig. 1d). Thus, we demonstrated that the effect of the two drugs in combination was not simply additive but synergistic, which highlighted the advantage of their combination.

**Molecular features of AD are improved by ABC *in vitro*.** Mitochondrial dysfunction is believed to play a critical role in AD pathology<sup>23</sup> triggering apoptosis. We sought to check whether





neuronal protection by ABC mechanistically involves the improvement of this dysfunction. We found that  $A\beta_{1-42}$  oligomers increased the release of mitochondrial cytochrome *c* into the cytoplasm (Fig. 2a), which was accompanied by caspase 3 activation (Fig. 2b) leading to apoptosis, but ABC was able to protect intoxicated neuronal cells from this apoptotic activation (Fig. 2). Oxidative stress is associated to mitochondrial dysfunction and plays a role in the development of AD pathology<sup>24</sup>. We assessed oxidative stress by measuring the levels of methionine residues oxidation (MetO) in neurons and showed that ABC significantly protected neuronal cells against such stress (Fig. 3a). The presence of toxic  $A\beta$  species in the brain of AD is believed to bring excessive glutamate accumulation<sup>25</sup> affecting synapse integrity<sup>8</sup> and triggering loss of neuronal cells. We demonstrated *in vitro* that ABC was able to diminish this  $A\beta_{1-42}$ -induced toxic glutamate increase (Fig. 3b). Tau protein hyperphosphorylation that brings its abnormal cellular distribution and aggregation into neurofilamentary tangles<sup>26</sup> is another important molecular feature of AD disease. It is believed to be an additional toxic factor leading to brain degradation in AD patients<sup>27</sup>. We found, that ABC was able to prevent Tau hyperphosphorylation induced by  $A\beta_{1-42}$  in cellular cultures (Fig. 3c).

Synaptic loss is prominent in affected brains and is largely responsible for the deterioration of the cognitive function. In neuronal cultures,  $A\beta_{1-42}$  oligomers induced a substantial synaptic loss, but ABC prevented this loss (Fig. 3d) further explaining the observed neuroprotection.

In all *in vitro* experiments above, we used BDNF exclusively as a positive control for quality control purposes.

**Molecular targets important for ACP and BCL mechanism of action in neuroprotection against  $A\beta$  toxicity.** In order to confirm our hypothesis that elements in the excitatory glutamatergic system as

well as the regulation through GABA and glycine receptor systems are playing a role in the neuroprotection against  $A\beta$  toxicity, we tested the relevance of some plausible targets in these pathways through a pharmacological approach. CGP54626, orthosteric antagonist of GABA<sub>B</sub> receptors, was able at nontoxic doses to block the neuroprotective effect of racemic BCL (Fig. 4a), which confirms the importance of GABA<sub>B</sub> receptor activation for the neuroprotective action of BCL. When strychnine, an antagonist of inhibitory glycine-gated channels, was used with ACP, it was also able to reverse the neuroprotective effect (Fig. 4b), pointing to the mediation of neuroprotection induced by ACP through its agonistic effect on ionotropic glycine receptors. On the other hand, similar experiments with the agonists DHPG and APDC, acting on group I and II metabotropic glutamate receptors respectively, clearly demonstrated the importance of the antagonistic effect of ACP on these molecular targets in excitatory glutamatergic transmission (Fig. 4c,d). Taken together, these results confirm the activity of our drugs on multiple receptors implicated in the GABAergic/glycinergic and glutamatergic signalling systems.

**ABC alleviates cognitive deficits in AD *in vivo* models.** To explore the effects of ABC in a functional context, we used a well-known model of intracerebroventricular injection of  $A\beta_{25-35}$  oligomers in mice to mimic both the cognitive impairment and the associated cellular degeneration observed in AD<sup>28,29</sup>.  $A\beta_{25-35}$  oligomerises in a similar manner to the larger  $A\beta_{1-42}$  peptide, forming  $\beta$ -sheet amyloid-like short fibrils and induces toxicity with a similar pattern<sup>30</sup>. Oligomeric preparations used in our study have been extensively characterised by us for the presence of toxic oligomers<sup>29,30</sup>, and were confirmed to produce AD-like symptoms *in vivo*<sup>30</sup>.  $A\beta_{25-35}$ , a fragment present in  $A\beta_{1-42}$ , was used for *in vivo*

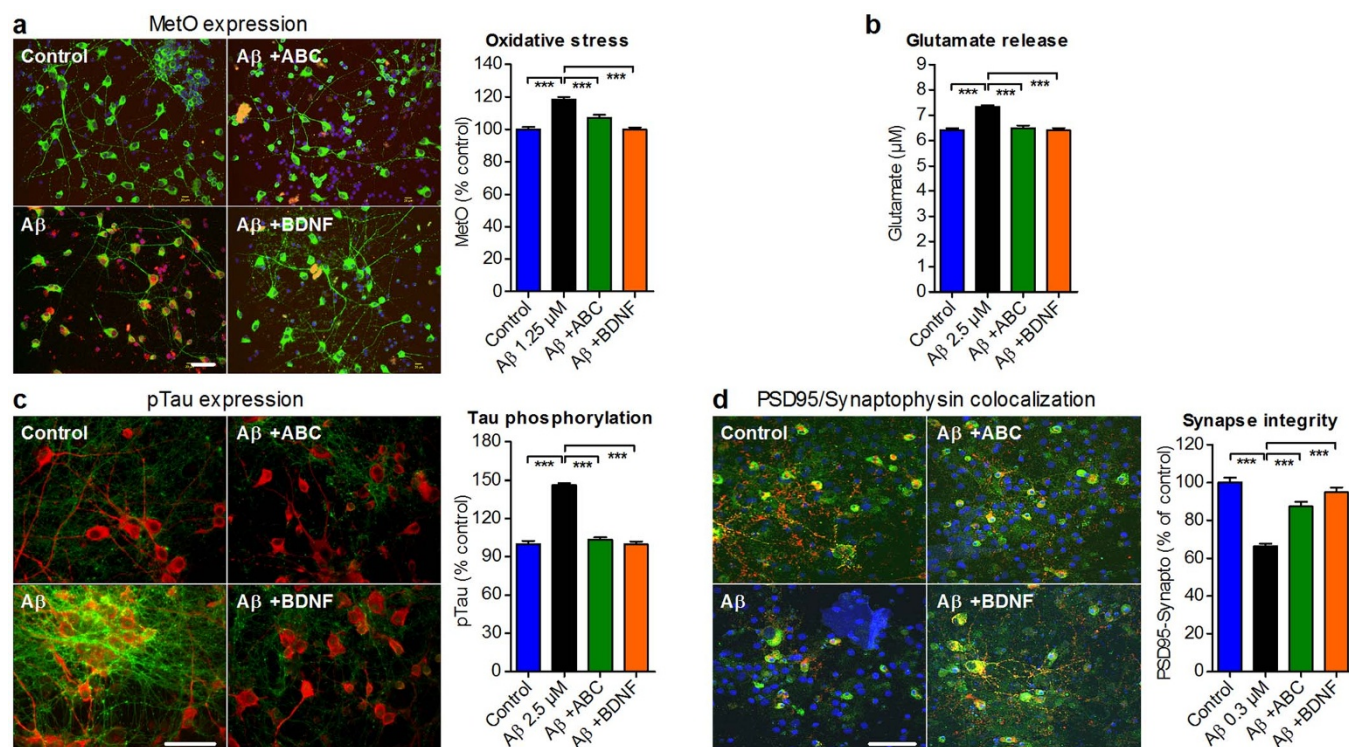


**Figure 3** | ABC protects  $A\beta_{1-42}$ -intoxicated neuronal cells from apoptosis by normalising several induced alterations. (a) ABC reduced oxidative stress as assessed by MetO staining. Neurons with MetO (in red) overlapping with MAP2 (in green) were counted and results were expressed as percentage of untreated control. (b) Normalisation by ABC of cell-released glutamate quantified in the medium of  $A\beta$ -intoxicated neurons. (c) Preservation by ABC of phosphorylated tau protein (pTau<sup>Ser212/Thr214</sup>, green) quantified in  $A\beta$ -intoxicated neurons (red). (d) Synaptic integrity was preserved following ABC treatment, as assessed by the co-localisation of pre-synaptic synaptophysin (red) and post-synaptic PSD95 (green) proteins. Scale bars: 60  $\mu$ m. Values are mean  $\pm$  s.e.m. \*\*\* $P < 0.001$  versus  $A\beta$ ; ANOVA with Dunnett's test. ABC was composed of 0.32 nM ACP and 80 nM BCL. BDNF was used as positive control (50 ng mL<sup>-1</sup>). MetO: Oxidised methionines; PSD95: Post-synaptic density protein 95. Blue: Hoechst.

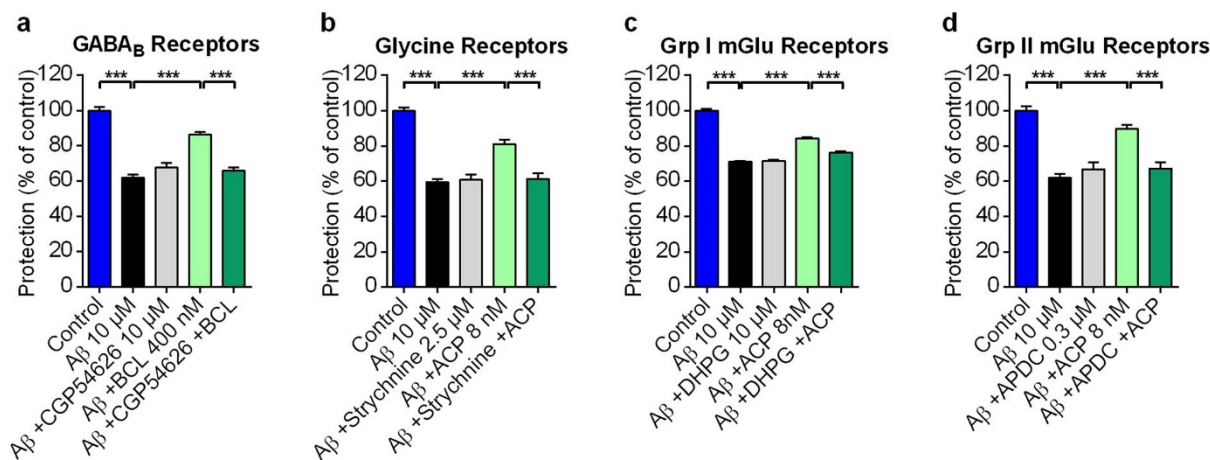


**Figure 4 | ACP and BCL act through GABA<sub>B</sub>, Glycine and metabotropic glutamatergic receptor signalling.** GABA<sub>B</sub>R CGP54626 antagonist (a), Glycine receptor Strychnine antagonist (b), mGluR1/5R DHPG agonist (c) and mGluR2/3R (2R,4R)-APDC agonist (d) all blocked BCL and ACP protection of rat primary neuronal cells validating the action of these drugs on these pathways. Values are mean  $\pm$  s.e.m. \*\*\* $P < 0.001$  versus A $\beta$ , BCL or ACP; ANOVA with Dunnett's test. mGlu1/5R and mGlu2/3R: metabotropic glutamate group I and II receptors respectively.

intracerebroventricular intoxications because it is more diffusible due to its smaller size. It was shown to penetrate in brain structures and produce a lasting toxic effect of over 6 weeks<sup>30</sup> only after one injection, unlike A $\beta$ <sub>1–42</sub> with its toxic effect on memory recovering after 10 days<sup>31</sup>. A $\beta$ <sub>25–35</sub> has been shown to have multiple biochemical effects on intracellular compartments similar to what is observed in AD patients<sup>32</sup>. Moreover, production of endogenous A $\beta$ <sub>1–42</sub> peptides could be easily and specifically monitored in A $\beta$ <sub>25–35</sub>-injected mice with the help of selective antibodies for the A $\beta$ <sub>1–42</sub> forms. The same batches of oligomerised A $\beta$ <sub>25–35</sub> peptides as well as control, nontoxic Sc.A $\beta$  peptides with the same amino acid composition were used in our study as described by Zussy *et al.*<sup>30</sup>. ACP and BCL dose selection was based on pharmacokinetics studies and modelling for the translation of drug concentrations effective *in vitro* to animal doses. For all tests below, treatment durations are detailed in Supplementary Table 2.

The effect of the combination of ACP and BCL at the selected doses was first assayed in the Morris Water Maze (MWM) test, which explores hippocampal-dependent spatial memory<sup>33</sup>, a form of memory affected early in AD. ABC showed a significant protection against cognitive impairment due to A $\beta$ <sub>25–35</sub> injury in the acquisition of long-term memory (Fig. 5a), as well as in the short-term memory test (Fig. 5b). We also used the novel object recognition (NOR), another memory task affected by hippocampal and cortical-mediated alterations<sup>34</sup>. A $\beta$ <sub>25–35</sub>-injected mice demonstrated deficits in NOR, while upon ABC treatment, the animals substantially and significantly recovered the ability to recognise novel objects (Fig. 5c). ABC was also able to restore this capacity in an analogous rat model assayed in another laboratory (Supplementary Fig. 2). Further, we evaluated ABC action in spontaneous alternation Y-maze test, which is partly linked to the septo-hippocampal system implicated in learning and spatial working memory<sup>35</sup>. In this test, ABC also substantially and significantly reversed alternation deficit induced by A $\beta$ <sub>25–35</sub> (Fig. 5d). Finally, we tested ABC in a passive avoidance test used to assess hippocampal and amygdala dependent aversive memory in animals<sup>36</sup>. ABC fully restored memory deficits induced by A $\beta$ <sub>25–35</sub> in this assay (Fig. 5e).

A cognitive decline is also observed in mouse transgenic models of AD<sup>37</sup> that possibly mimics some aspects of the prodromic phases of human disease. At the age of 8 months, when *hAPP*<sub>SL</sub> transgenic mice cognition was already impaired, we treated animals for 3–4 weeks with ABC and found a substantial improvement of cognitive deficits assessed by MWM acquisition and working memory tests (Fig. 5f,g).

Since ABC showed synergism between drugs *in vitro*, we then tested ACP, BCL and ABC in the Y-maze test in a dose-dependent fashion in the acute peptide injection model. We observed a limited activity for ACP or BCL alone for certain doses, but the ABC effect was dose-related and consistently and significantly stronger (Supplementary Fig. 3), demonstrating a formal synergistic interaction between these two drugs *in vivo* as well (Fig. 5h). We found that ABC did not affect the basal cognition of age-matched naive mice and mice injected with control A $\beta$ <sub>25–35</sub> scrambled peptide (Supplementary Fig. 4), showing the limitation of action of ABC treatment to the pathological condition induced in this model by A $\beta$ <sub>25–35</sub>.

**Mechanistic aspects of ABC regarding its action on the functional preservation *in vivo*.** ABC proved its potential to alleviate A $\beta$ <sub>25–35</sub>-induced cognitive deficits *in vivo* in several models and memory paradigms. To understand what brought the beneficial effect of ABC on cognition, we addressed several changes relevant to the human disease. First, we asked whether brain integrity is preserved by ABC and looked for BBB alterations after acute injection of A $\beta$ <sub>25–35</sub>. Following ABC treatment, BBB was preserved in injured mice as assessed by systemic injection of Evans Blue dye and quantification in brain (Fig. 6a). Hippocampus is one of the main regions of the brain affected at the early stages of AD and it is severely compromised in the A $\beta$ <sub>25–35</sub> acute injection model<sup>28,29</sup>. When A $\beta$ <sub>25–35</sub>-injured animals were treated with ABC, CA1 neurons were substantially and significantly preserved (Fig. 6b). Since CA1 loss in AD could be a consequence of oxidative stress and apoptosis<sup>38</sup>, we also tested the ability of ABC to normalise these alterations induced by A $\beta$ <sub>25–35</sub> *in vivo*. We found that ABC prevented lipid peroxidation (Fig. 7a), a marker for such stress, and protected neuronal cells from apoptosis as assessed by cleaved poly-ADP-ribose polymerase level (cPARP)<sup>39</sup> (Fig. 7b).

Another feature of AD is neuroinflammation<sup>40</sup> accompanied by elevated levels of pro-inflammatory lymphokines released by activated microglia. To examine the effect of ABC on this inflammatory process, we quantified the proinflammatory cytokines TNF $\alpha$  and IL-1 $\beta$  and found their levels to be reduced to normal upon ABC treatment (Fig. 8a,b). One of the described consequences of brain degeneration and neuroinflammation in AD is glial scarring<sup>41</sup>. When A $\beta$ <sub>25–35</sub>-injured mice were treated with ABC, we found that gliosis was normalised (Fig. 8c).

Accumulation of endogenous oligomeric A $\beta$ <sub>1–42</sub> is one of the toxic factors responsible for symptoms observed in AD<sup>42</sup>. Its toxicity could mediate many of the alterations described above or be amplified by



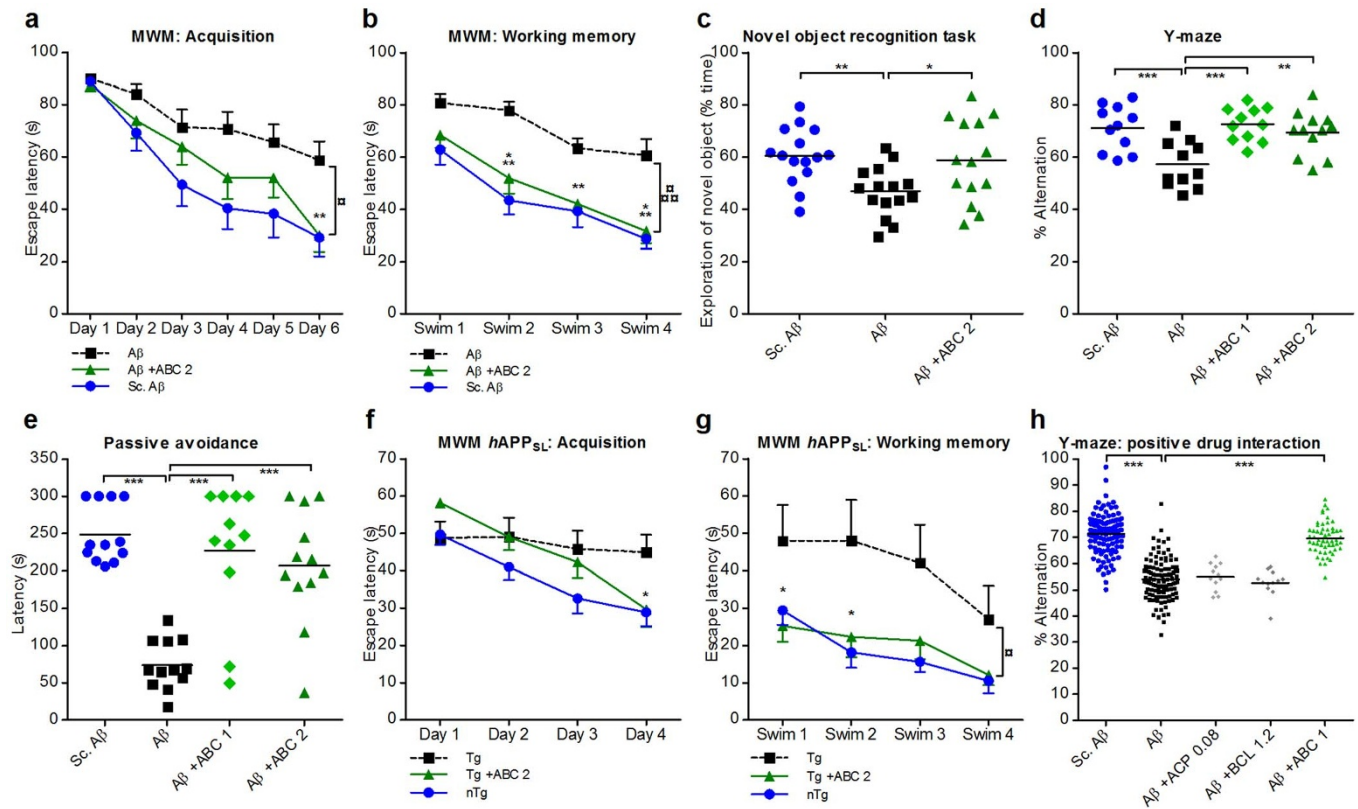


**Figure 5 | ABC alleviates cognitive deficits in AD mouse models.** Intracerebroventricularly  $A\beta_{25-35}$ -injected Swiss male mice compared to Sc.A $\beta$  controls: Positive effect of ABC in the Morris Water Maze (MWM) acquisition task (a) and working memory tests (b) ( $n = 12$ ). Positive effect of ABC in NOR task (c) ( $n = 15$ ), and in representative Y-maze (d) and passive avoidance (e) experiments ( $n = 12$ ). Locomotor activities of Sc.A $\beta$ , A $\beta$ , and treated mice were unchanged in Y-maze and NOR tests (Supplementary Fig. 5). Transgenic  $hAPP_{SL}$  C57BL/6 male mice: Positive effect of ABC in MWM acquisition (f) and working memory tests (g) ( $n = 12$ ). (h) ABC superior activity over its single drugs (combined analysis (see Supplementary Fig. 3)). Values are mean  $\pm$  s.e.m. \* $P < 0.05$ , \*\* $P < 0.01$ , \*\*\* $P < 0.001$  versus A $\beta$  (c–e,h) (ANOVA with Dunnett’s test) or ABC versus A $\beta$  (a,b) and ABC versus Tg (f,g) (mixed ANOVA with Dunnett’s test). <sup>oo</sup> $P < 0.01$ , <sup>ooo</sup> $P < 0.001$  global ABC versus global A $\beta$  (a,b), or global ABC versus global Tg (f,g) (mixed ANOVA with Dunnett’s test). ABC 1: ACP 0.08 mg Kg<sup>-1</sup> + BCL 1.2 mg Kg<sup>-1</sup>; ABC 2: ACP 0.2 mg Kg<sup>-1</sup> + BCL 3 mg Kg<sup>-1</sup>. ■: A $\beta$  (a,b) or Tg (f,g); ▲: A $\beta$  (a,b) or Tg (f,g) + ABC 2; ●: Sc.A $\beta$  (a,b) or nTg (f,g). Tg: transgenic; nTg: nontransgenic. Sc.: scrambled.

them. When mice were exposed to exogenous  $A\beta_{25-35}$ , we observed a substantial and significant increase in endogenous  $A\beta_{1-42}$ , confirming the previously reported findings<sup>43</sup> and suggesting a positive feedback loop in the formation of toxic A $\beta$  species. This overproduction was fully and significantly normalised by ABC treatment (Fig. 9a). As synaptic alterations observed in AD could result from the accumulation of toxic A $\beta$  oligomers, we tested ABC for its ability to preserve synaptic loss. When synaptophysin marker was used to this goal we observed its substantial and significant normalisation (Fig. 9b). Another important consequence of  $A\beta_{1-42}$  accumulation is dysregulation in the amount of brain-derived neurotrophic factor (BDNF). This factor is thought to undergo a compensatory increase under conditions of A $\beta$ -associated neurotoxicity<sup>44</sup>, that is supposed to aid in neuronal protection. We confirmed that the level of BDNF was significantly increased in  $A\beta_{25-35}$ -injured mice, but it was maintained at normal levels by ABC treatment (Fig. 9c) that probably acted upstream of the BDNF compensatory induction.

When we compared the effect of single drugs to that of ABC for several biochemical features, we observed the same strong positive interaction between ACP and BCL that we demonstrated before in the Y-maze memory paradigm (Supplementary Fig. 3 and Fig. 5h). It was evident from synergistic effects on apoptosis, inflammation (IL-1 $\beta$ ), endogenous  $A\beta_{1-42}$  accumulation, synapse integrity and BDNF levels (Figs 6 to 9).

## Discussion

The multifactor nature of AD might be one of the reasons why past mono-therapeutic attempts were not particularly effective. The

underlying idea of our approach was to explore the possibility of developing combination therapy acting downstream of the formation of toxic A $\beta$  species that might robustly prevent the degradation of both neuronal and endothelial cellular structures affected in this disease. We therefore considered that such treatment could potentially have a disease modifying effect. We were guided by the fact that many signalling pathways are pleiotropic<sup>45</sup>, which opens up the possibility of designing new treatments based on approved drugs acting on them. In combination, such drugs might lead to an enhanced therapeutic effect at a lower dosage<sup>46</sup>, further decreasing the risk of potential undesirable events.

Our analysis of regulators acting on interconnected signalling pathways led to two well-known drugs with rather favourable safety profile: BCL and ACP. Some of their targets are well documented, while the action on others could be indirect and dose specific, especially in the case of ACP usually used at extremely high doses. Metabotropic GABA<sub>B</sub> receptors play a fundamental role in controlling the degree of neuronal activity. At glutamatergic synapses, pre-synaptic GABA<sub>B</sub> heteroreceptors can decrease the release of glutamate from the presynaptic membrane by inhibiting Ca<sup>2+</sup> channels, while postsynaptic GABA<sub>B</sub> receptors attenuate excitatory currents by activating Kir3-type K<sup>+</sup> channels<sup>47</sup>. Therefore, we suppose that activation of GABA<sub>B</sub> receptors by agonistic action of BCL can restore the disequilibrium induced by the dysregulation in glutamatergic signalling that is provoked by neurotoxic forms of A $\beta$ . Additionally, activation of GABA<sub>B</sub> receptors by BCL could attenuate, via IGF-1 receptor, the pro-apoptotic signalling specifically

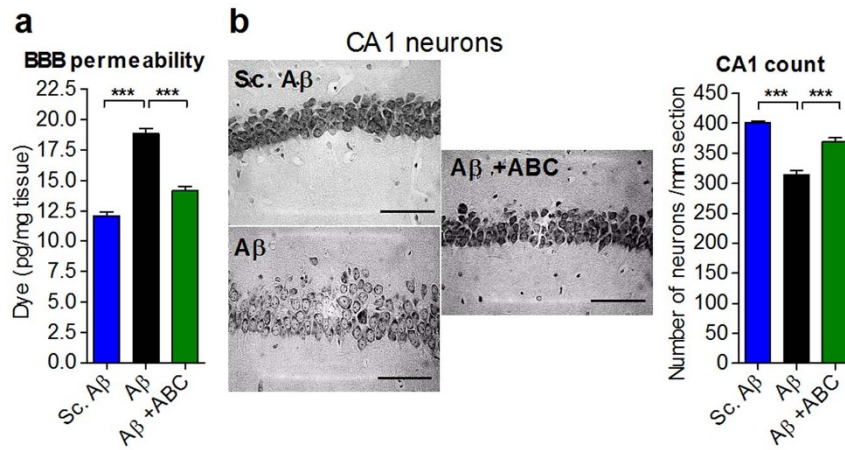


**Figure 6** | ABC preserves phenotypic alterations occurring *in vivo* in A $\beta_{25-35}$ -injected animals. ABC protected the BBB from leakage as assessed by Evans Blue dye in brain after systemic injection (a) ( $n = 12$ ), and preserved hippocampal CA1 pyramidal cells (b) ( $n = 12$ ). (b) Representative images of Cresyl violet-stained hippocampal CA1 neurons before and after ABC treatment. Hippocampal CA1 pyramidal cells were counted from 8 slices per animal and 6 mice per group and results were expressed as number of neurons per mm. ABC was composed of ACP 0.2 mg Kg<sup>-1</sup> and BCL 3 mg Kg<sup>-1</sup>. Values are mean  $\pm$  s.e.m. \*\*\* $P < 0.001$  versus A $\beta$ ; ANOVA with Dunnett's test. Sc.: scrambled.

engaged by neurotoxic A $\beta$  protein<sup>48</sup>. Inhibitory receptors like GABA<sub>B</sub> are also present in endothelial cells, suggesting that the balance between excitatory and inhibitory neurotransmitters could play an important role not only in the regulation of brain functions, but also in the functioning of the vascular system<sup>49,50</sup>. Therefore, activation of inhibitory GABA<sub>B</sub> receptors can be recognised as a promising therapeutic strategy for decreasing excessive activity of glutamatergic signalling and restoring E/I balance. In our study, we were able to confirm the strong neuroprotective effect of BCL *in vitro*. This effect disappeared in the presence of orthosteric antagonist of GABA<sub>B</sub> receptors, experimentally confirming the on-target agonistic action of BCL in this model. The second drug, ACP (calcium salt of acetyl homotaurine), was first approved in 1989 and since then has been used to treat millions of alcohol-dependent patients worldwide<sup>51</sup>. It was shown to reduce relapse in alcohol-dependent patients through restoration of the balance between excitatory and inhibitory transmission affected by chronic alcohol use. ACP could decrease glutamate level in human brains, induced by hyperexcitability during

episodes of ethanol withdrawal<sup>12</sup>. It is supposed to attenuate hyper-glutamatergic states that occur during abstinence, via inhibitory effects on glutamate receptors and potentiation of inhibitory neuronal signalling. However, its precise mechanism of action in addiction treatment remains largely unknown. Moreover, it has been suggested that at least a part of its effects can be due to the presence of calcium ions<sup>52</sup>. In our neuroprotection experiments, ACP has been effective in a fraction of nanomolar concentrations, excluding its effect due to the presence of calcium ions. Moreover, we demonstrated experimentally that ACP neuroprotective effect was specifically mediated by N-acetyl homotaurine (ACP) and not by calcium ions contained in its calcium salt (Supplementary Fig. 6).

Calcium ACP was shown to be a weak modulator of NMDA receptors<sup>53,54</sup>, but its action is probably not direct. Since sodium ACP did not compete with NMDA for glutamate binding sites but displayed total competition with trans-ACPD<sup>55</sup>, a nonspecific

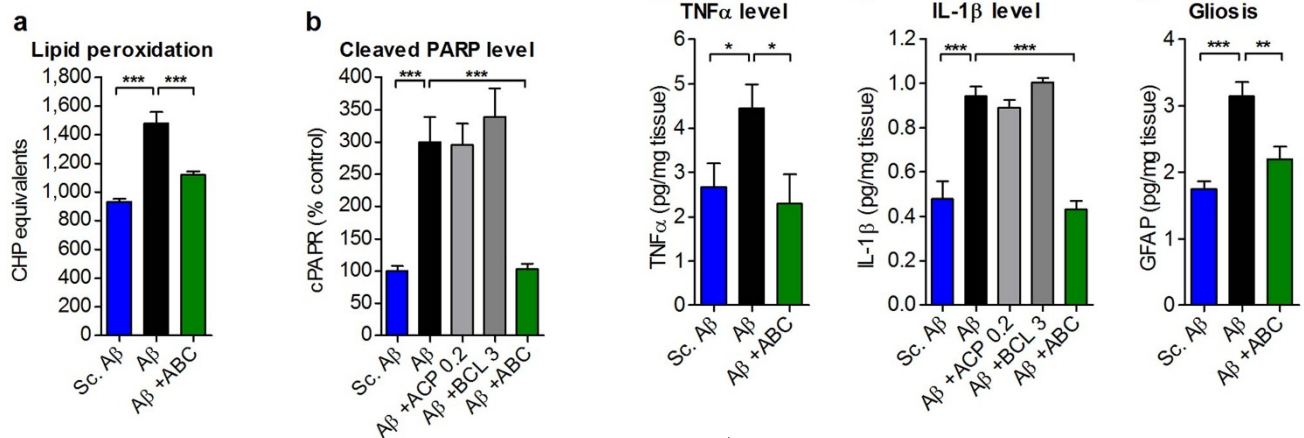


**Figure 7** | ABC protects from oxidative stress and apoptosis *in vivo* in A $\beta_{25-35}$ -injected animals. (a) Decrease in oxidative stress assessed by lipid peroxidation in mice hippocampi following ABC treatment ( $n = 6$ ). (b) cPARP levels were normalised by ABC in mice hippocampi ( $n = 6$ ). A higher efficacy was observed for ABC with respect to its single drugs. ABC was composed of ACP 0.2 mg Kg<sup>-1</sup> and BCL 3 mg Kg<sup>-1</sup>. Values are mean  $\pm$  s.e.m. \*\*\* $P < 0.001$  versus A $\beta$ ; ANOVA with Dunnett's test. CHP: cumene hydroperoxyde; Sc.: scrambled.

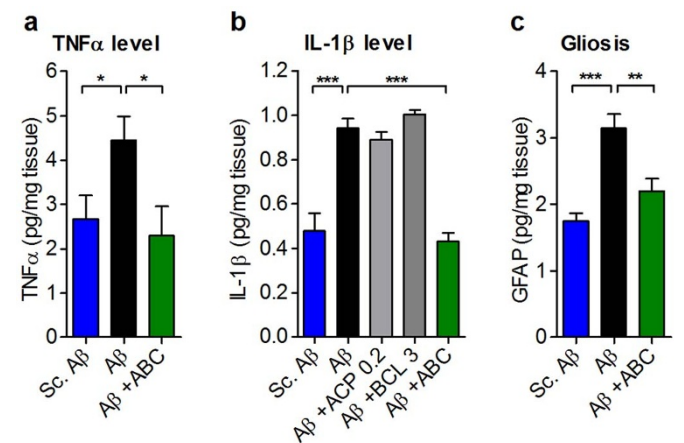


**Figure 8** | ABC normalises inflammation and gliosis *in vivo* in A $\beta_{25-35}$ -injected animals. Normalisation by ABC of TNF $\alpha$  (a) and IL-1 $\beta$  (b) protein levels in mice hippocampi ( $n = 6$ ). A higher efficacy was observed for ABC with respect to single drugs. (c) Gliosis, assessed by GFAP protein quantification, was also normalised in mice hippocampi following ABC treatment ( $n = 6$ ). ABC was composed of ACP 0.2 mg Kg<sup>-1</sup> and BCL 3 mg Kg<sup>-1</sup>. Values are mean  $\pm$  s.e.m. \* $P < 0.05$ , \*\* $P < 0.01$ , \*\*\* $P < 0.001$  versus A $\beta$ ; ANOVA with Dunnett's test (except in (a), *t*-test). GFAP: glial acidic fibrillary protein; Sc.: scrambled.



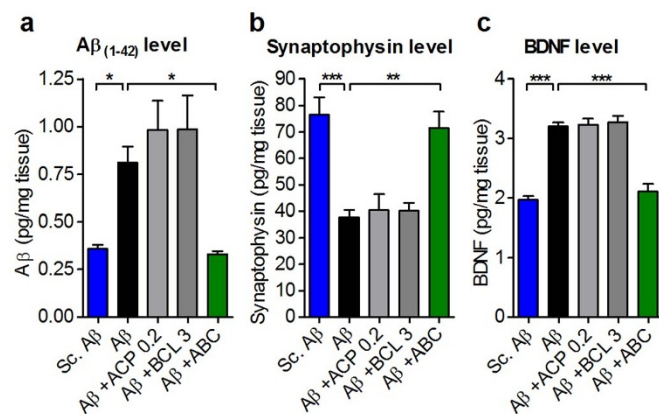


**Figure 9** | ABC protects from  $A\beta_{1-42}$  accumulation and synaptic loss, and from consequent downstream BDNF deregulation *in vivo*. ABC protected from  $A\beta_{1-42}$  endogenous secretion in mice hippocampi (a) ( $n = 6$ ) preserving synapse integrity assessed by synaptophysin protein quantification (b) ( $n = 6$ ). (c) BDNF protein level was normalised in mice hippocampi following ABC treatment ( $n = 6$ ). A higher efficacy was observed for ABC with respect to single drugs. ABC was composed of ACP 0.2 mg  $Kg^{-1}$  and BCL 3 mg  $Kg^{-1}$ . Values are mean  $\pm$  s.e.m. \* $P < 0.05$ , \*\* $P < 0.01$ , \*\*\* $P < 0.001$  versus A $\beta$ ; ANOVA with Dunnett's test. Sc.: scrambled.

agonist for group I and II metabotropic glutamate receptors (mGluRs), we decided instead to evaluate a role of metabotropic glutamate receptors for neuroprotective effects observed by us. The role of these receptors in the pathogenesis of AD is not yet fully established, and published observations are limited. mGluR2, belonging to group II glutamate receptors, was found to be overexpressed in the hippocampus of AD patients<sup>56</sup>. Caraci *et al.* demonstrated that a positive allosteric modulator of group II mGluR2 aggravated A $\beta$ -induced neurotoxicity<sup>57</sup>, while knockout of group I mGluR5, considered as a co-receptor for A $\beta$ <sup>58</sup>, attenuates cognitive impairment in a mouse model of AD<sup>59</sup>. APP has been shown to be rapidly translated in the synapses in response to DHPG, agonist of group I mGluRs<sup>60</sup>, and such activation stimulates the release of A $\beta_{1-42}$  in cortical synaptoneuroosomes in a mouse model of AD, while stimulation of group II mGluRs triggers production and release of both A $\beta_{1-42}$  and A $\beta_{1-40}$ <sup>61</sup>. By a pharmacological approach with the help of two broadly specific agonists, we demonstrated experimentally that the neuroprotective action of ACP is mediated by its antagonistic effect on both group I and group II mGluRs.

In the ethanol addiction model, ACP has been shown to act in the nucleus accumbens through agonism on glycine receptors (GlyRs)<sup>16</sup>. These inhibitory channels are expressed throughout all regions of the hippocampus<sup>62</sup>. At the synapses, they are co-localised with GABA<sub>A</sub> receptors but mostly are found in extrasynaptic sites. In our experiments, we demonstrated that neuroprotection by ACP is also mediated by its agonistic action on GlyR channels. We hypothesise that activation of GlyRs by ACP might be an important factor for the attenuating excessive/aberrant neuron excitability, such as deleterious over-activation of extrasynaptic NMDA receptors by A $\beta$ <sup>8</sup>. These experiments suggested that, for the neuroprotective action of ACP against A $\beta_{1-42}$  toxicity, its antagonistic signalling through both Group I and group II metabotropic glutamate receptors as well as agonistic activation of GlyR channels is required, while BCL action is mediated by activation of GABA<sub>B</sub> receptors. Yet, our data is not conclusive at this stage but we suppose that neuroprotective effects of ABC could be mediated by a serial signalling cascade involving all these receptors. Future work is needed to further characterise the mode of action of ABC in this regard as well as its specificity on our studied targets.

While no comprehensive model for Alzheimer's disease exists<sup>20</sup>, representing the major limitation for the discovery of effective drugs, multiple observational endpoints relevant to the human disease were improved by ABC in several cellular and animal paradigms modelling different aspects of AD. *In vitro*, ACP and BCL proved to be cytoprotective both for neurons as well as for vascular cells with strong synergistic effect and at relatively low doses. The exact mechanisms explaining such action are only emerging, but we found that neuroprotection could be due to the down-regulation of glutamate release, tau phosphorylation and diminished oxidative stress, and that it is mediated by an antagonistic action on metabotropic receptors of classes I/II and an agonistic action on GlyR in the case of ACP, and activation of GABA<sub>B</sub>R in the case of BCL.

The acute model of intracerebroventricular injection of A $\beta$  peptide into healthy rodents mimics main features of AD-type dementia including neuronal degeneration, cognitive deficits accompanied by hippocampal dysfunction<sup>28</sup> and BBB impairment<sup>63</sup>. Since cognitive function and memory do not have a complete analogy between rodents and humans, we tested the influence of our drug combination in several memory paradigms. We observed a strong and synergistic improvement of cognition accompanied by substantial neuronal protection and BBB preservation. The important biochemical landmarks (A $\beta_{1-42}$ , oxidative stress, inflammation) of AD were significantly diminished by the drug combination. The effect was not due to a simple memory enhancement since in animals injected with nonspecific scrambled A $\beta$  peptide as well as in normal animals cognition was not affected by ABC. In addition, ABC proved to be effective when tested in the transgenic mouse model at a stage when cognitive functions were already altered. Together, all these results open the possibility that ABC could exert a disease modifying effect. Already, we demonstrated that several patterns altered in AD, such as glutamate accumulation, tau hyperphosphorylation, endogenous A $\beta$  oligomers and synaptic loss were synergistically normalised by ABC.

Our results demonstrate the value of 1) the combinational approach and 2) using for this purpose previously existing drugs in new combinations<sup>11</sup>. Many new drugs effective in preclinical models failed in human trials due to their toxic effects, while ACP and BCL have been used for a long time to treat patient populations and demonstrated very limited degree of side effects. The synergistic potency of the combination could allow further reduction of therapeutic doses and thus lower the risk for side effects. Indeed, we consistently observed a positive effect at low doses as we progressed from *in vitro* studies to animal models. Over 200 compounds have been shown to affect favourably AD-like pathology in experimental models<sup>64</sup>. However, to our knowledge, none of them have shown a simultaneous *in vitro* and *in vivo* improvement of the number of diverse biological AD related features as our combination. It protected both neuronal and vascular brain cells from A $\beta$  insults, preserved synapses and reduced excessive tau protein phosphorylation, while at the same time reduced soluble endogenously produced A $\beta$  peptides, diminished the signs of neuroinflammation and gliosis and alleviated cognitive deficits in different memory paradigms in AD animal models. We consider that the integrity of our data suggest that ABC might be a valuable disease-modifying treatment for AD, acting through a new mechanism implicating multiple molecular targets. If confirmed by powered clinical testing, low-dose ABC could serve as a basis for a new conceptual approach for Alzheimer's disease therapy and also might help to understand the underlying mechanisms of this devastating dementia.

## Methods

**Animals.** All animal procedures were carried out in strict adherence to the European Community Council Directive of September 22, 2010 (2010/63/UE). All experiments and protocols were authorised and approved by the French Ministry of Research, as well as by Animal Welfare Committees of Amylgen, Biotrial, QPS and Neuronexperts. All efforts were made to minimise the number of animals used. Male Swiss mice (Janvier, Saint Berthevin, France) aged 4–6 weeks and weighing



25–32 ± 2 g, and male Sprague Dawley rats (Janvier) aged 7–8 weeks weighing 220–300 g were used for Aβ<sub>25–35</sub> intoxications. For transgenic mice experiments, male mice overexpressing the 751 amino acid form of human APP (hAPP) with London (V717I) and Swedish (KM670/671N/L) mutations (hAPP<sub>SL</sub>) under the control of the murine Thy-1 promoter<sup>65</sup> were bred at QPS (Austria), and C57BL/6 age and gender matched transgenic littermates served as controls (nTg). Animals were housed in plastic cages with free access to food and water, except during behavioural experiments, and kept in a regulated environment (23 ± 1°C, 50–60% humidity) under a 12 h light/dark cycle. For *in vitro* experiments, female Wistar rats (Janvier) on gestational day 15 were killed by cervical dislocation and foetuses were removed from the uterus.

**Drugs and treatments.** Aβ<sub>1–42</sub> peptide (Bachem, Reference H1368, Batch 1010533) was prepared in serum-free culture medium (0.1% DMSO) at 40 μM and was slowly shaken at +37°C for 3 days in the dark. After 3 days, Aβ<sub>1–42</sub> oligomers were used on primary cortical neurons at specified concentrations and for indicated incubation times depending on the assay (Supplementary Table 1). It is worthy of note that, for *in vitro* and *in vivo* experiments, when a new batch was selected, Aβ preparations were always verified for the presence of Aβ oligomers. In dose-response studies *in vitro*, these preparations were tested using the appropriate reference compounds such as BDNF and β-estradiol (which rescue Aβ toxic effect) to check for reproducibility between studies. In addition, we note that our Aβ<sub>1–42</sub> oligomeric preparation was performed in media containing phenol red at concentrations (i.e. 44 μM) that did not affect oligomeric formation as assessed by Western blot analyses attesting for the presence of these toxic oligomers<sup>21</sup> that were active in our experimental settings. It was also described elsewhere that high concentrations of phenol red should be used over several days to inhibit efficiently Aβ<sub>42</sub> oligomerisation<sup>66</sup>.

The amyloid-β[25–35] peptide (Aβ<sub>25–35</sub>) and scrambled control Aβ<sub>25–35</sub> (Sc.Aβ) peptide were purchased from Genepep (Saint-Jean-de-Védas, France) for mice and from Bachem (Germany) for rat experiments. Peptides were solubilised in distilled water at a concentration of 3 mg mL<sup>-1</sup> (mice) or 2 mg mL<sup>-1</sup> (rats) and stored at -20°C until use. Before injection, peptides were incubated at +37°C for 4 days, allowing Aβ<sub>25–35</sub> to form oligomers. A quality control analysis for Aβ<sub>25–35</sub> aggregation was systematically performed by light scattering analysis before each injection of Aβ<sub>25–35</sub> peptides. 9 nmol per mouse or 15 nmol per rat of Aβ<sub>25–35</sub> peptide or Sc.Aβ were administered once *in vivo* in a final volume of 3 μL per mouse or 8 μL per rat<sup>29</sup>.

(RS)-Baclofen and acamprostate calcium were provided by Sigma Aldrich. Acamprostate sodium was synthesised by NovAlix (Illkirch, France). Drugs were solubilised in distilled water and prepared before each administration. For *in vitro* studies, ACP, BCL or ABC dissolved in 0.1% DMSO were added 1 h or 48 h before Aβ<sub>1–42</sub> intoxication and maintained until the end of Aβ intoxication (Supplementary Table 1). For mechanism of action studies, non-toxic concentrations of CGP54626 (10 μM, GABA<sub>B</sub>R antagonist, Tocris Biosciences), Strychnine (2.5 μM, Glycine receptor antagonist, Tocris Biosciences), (S)-3,5-dihydroxyphenylglycine (DHPG, mGluR1/5 agonist 10 μM, Tocris Biosciences) and (2R,4R)-amino-2,4-pyrrolidinedicarboxylic acid (APDC, mGluR2/3 agonist, 0.3 μM, Sigma Aldrich) were dissolved in 0.1% DMSO (except for DHPG dissolved in water) and added 2 h (except for DHPG, 1 h) before ACP (8 nM) or BCL (400 nM) to rat primary neuronal cells.

To treat the animals, compounds were administered *per os* twice daily at 8:00 am and 6:00 pm in a volume of 5 mL Kg<sup>-1</sup> (mice) or 10 mL Kg<sup>-1</sup> (rats). Aβ<sub>25–35</sub> or Sc.Aβ was injected once for each experiment and treatment started 24 h before Aβ<sub>25–35</sub> or Sc.Aβ or injection and lasted until the end of behavioural tests (see behavioural analyses below and Supplementary Table 2). For hAPP<sub>SL</sub> mice, treatment was started at 8 months of age and lasted 3–4 weeks until the end of functional tests (Supplementary Table 2). All behavioural tests were performed 2 h after treatment.

**Cell cultures.** Cultures, Aβ<sub>1–42</sub> intoxications and treatments were validated and performed at Neuronexperts laboratories (Marseille, France). Rat primary cortical and hippocampal neurons were cultured as described previously<sup>21</sup>. Briefly, 3 pregnant Wistar female rats of 15 days gestation for the use of cortical neurons or 17 days gestation for hippocampal neurons were killed by cervical dislocation and cortices of foetuses were dissociated. Cells were then mechanically dissociated with trypsin 0.05% (Pan Biotech, Aidenbach, Germany) and suspended after washing in a defined culture medium consisting of Neurobasal medium supplemented with 2% B27 (Invitrogen, Cergy Pontoise, France), 2 mM L-glutamine (Pan Biotech), 2% of Penicillin/Streptomycin (PS) and 10 ng mL<sup>-1</sup> of brain-derived neurotrophic factor (BDNF, Pan Biotech). Cells were seeded in 96 well-plates pre-coated with poly-L-lysine (Greiner, Courtaboeuf, France) and were cultured at +37°C in a humidified air (95%)/CO<sub>2</sub> (5%) atmosphere. After 11–13 days of culture of cortical neurons, cells were pre-treated for 1 h with ACP, BCL or combination (ABC) and then intoxicated with the appropriate concentration of Aβ<sub>1–42</sub> during variable incubation times depending on the experiment (Supplementary Table 1). These different incubation times and concentrations were optimised to elicit only the toxic effects specific to the particular assay performed<sup>21</sup>. Seven different experiments with 18 replicates per experiment were performed and analysed. Hippocampal neurons were cultured during 18 days, then pre-treated for 48 h with ACP, BCL or ABC and finally intoxicated with Aβ<sub>1–42</sub> during 48 h. Three different cultures with 6 replicates each were performed and analysed.

Mycoplasma-free Human Brain Microvascular Endothelial Cells (HBMEC, ref ACBRI 376, Cells System, Illinois, USA) were rapidly thawed at +37°C and immediately suspended in 9 mL Dulbecco's modified Eagle's medium (DMEM; Pan Biotech) containing 10% of foetal calf serum (FCS; Invitrogen). Cell suspensions were centrifuged at 180 g for 10 min at +4°C and pellets were suspended in CSC serum-

free medium supplemented with 1.6% of Serum-free RocketFuel (Cell System), 2% of PS (Pan Biotech) and were seeded at the density of 20,000 cells per well in 96 well-plates (Matrigel Layer Biocoat Angiogenesis System, BD Biosciences, France) in a final volume of 100 μL (Supplementary Table 1). 3 different experiments with 18 replicates per experiment were performed and analysed.

**In vitro endpoint measurements.** Before performing experiments with our candidate drugs, we validated experimental conditions with BDNF (50 ng/mL) for neuronal cultures or VEGF (10 nM) for endothelial cultures as positive controls to check and confirm the restoration and the validity of each endpoint after Aβ<sub>1–42</sub> intoxication.

**Neuroprotection.** 24 h after Aβ<sub>1–42</sub> intoxication (Supplementary Table 1), culture supernatants were analysed with Cytotoxicity Detection Kit (LDH, Roche Applied Science, Meylan, France), a colorimetric assay based on the measurement of lactate dehydrogenase (LDH) released from the cytosol of dying cells, following the manufacturer's instructions.

**Methionine sulfoxide (MetO), cytochrome c (Cyto c), Caspase 3, phosphorylated Tau (pTau), PSD95 and Synaptophysin.** After Aβ<sub>1–42</sub> intoxication (Supplementary Table 1), cells were fixed, permeabilised, and non-specific sites were blocked with a solution of phosphate buffered saline (PBS; PanBiotech) containing 0.1% of saponin (Sigma) and 1% FCS. Then, cells were incubated with primary antibody, co-stained with the other primary antibody, and revealed with secondary antibodies (Supplementary Table 3). Nuclei were counter-stained with Hoechst (Sigma). 10 to 40 pictures per well were taken in each experiment using the InCell Analyzer<sup>TM</sup> 1000 (GE Healthcare, France). Analysis was done using Developer software (GE Healthcare) assessing the overlap between MAP2 on one side, and MetO, Cyto c, Caspase 3 or pTau staining on the other side. PSD95 and Synaptophysin total surface overlap was quantified (in μm<sup>2</sup>) and computed for each condition. Results were expressed as the number of overlapping stained cells per field and reported as a percentage of vehicle control.

**Glutamate release.** After 4 h of Aβ<sub>1–42</sub> intoxication (Supplementary Table 1), cell media supernatants were analysed with Amplex Red Glutamic Acid assay kit (Invitrogen) according to the manufacturer's instructions.

**Capillary network quantification.** 2 pictures with a 4× lens were taken per well using InCell Analyzer<sup>TM</sup> 1000 in light transmission. Analysis of the tube formation was done using Developer software and the total length of capillary network was computed.

**Behavioural analyses.** Animals were tested in a random and blind manner. Treatment groups were equally represented in each cage. Mice were habituated 30 min to 2 h before each experiment. Acute Aβ<sub>25–35</sub> injection experiments (Supplementary Table 2) and readouts as well as novel object recognition studies were done and validated at Amylgen facilities (Montferrier-sur-Lez, France) for mice, and at Biotrial (Aβ<sub>25–35</sub> experiments only) laboratories (Rennes, France) for rats. Transgenic mice studies were performed and validated at QPS facilities (Austria). Sample sizes used for behavioural analyses were also determined in each of these companies on the basis of previous experience on assay variability. Dead mice and mice that did not succeed preliminary control tests (i.e. very weak locomotor activity) were excluded from whole analyses.

**Place learning in the Morris Water Maze<sup>67</sup>.** Briefly, swimming was recorded using a Videotrack software (Viewpoint, Champagne-au-Mont-d'Or, France), with trajectories being analysed as latencies and distances. The software divides the pool into four quadrants. Training consisted in three swims per day for 6 days, performed between day 7 and 12 after Aβ<sub>25–35</sub> injection, with 20 min between each swim. For hAPP<sub>SL</sub> mice, training consisted in 4 swims per day for 4 days. The latency, expressed as mean ± s.e.m., was calculated for each training day. A probe test was performed 24 h after the last swim, on day 13 after Aβ<sub>25–35</sub> injection (retention phase). The platform was removed and each animal was allowed a free 60 s swim. The time spent in each quadrant was then determined. From Day 14 to 16 after Aβ<sub>25–35</sub> injection, or after the training test performed in hAPP<sub>SL</sub> mice, animals were tested for spatial working memory. Working memory was specifically assayed by changing the platform location everyday (four swims per day during 3 days) and by using a training inter-trial time of 2 min. The swimming times to find platform of first (swim1), second (swim2), third (swim3) and fourth trial (swim4) of every day were calculated and averaged in Aβ<sub>25–35</sub> mice experiments. In hAPP<sub>SL</sub> mice experiments, only data of day 2 trial were used.

**Novel object recognition<sup>34</sup>.** Briefly, 6 days after Aβ<sub>25–35</sub> or Sc.Aβ peptide injection, mice were placed individually in a squared open-field and their locomotor activity was captured through an IR-sensitive camera and analysed using the Videotrack<sup>®</sup> software (Viewpoint) in terms of total distance travelled (cm). 24 h later (7 days after Aβ<sub>25–35</sub> injection), two identical objects were placed at defined positions. Each mouse was placed in the open-field and the exploratory activity recorded during 10 min. The duration of contact with objects was analysed using the Nosetrack<sup>®</sup> protocol (Viewpoint). 24 h later (8 days after Aβ<sub>25–35</sub> injection), the object in position #1 was replaced by a novel one differing in colour, shape and texture from the familiar object. Each mouse was placed again in the open-field and the exploratory activity recorded during 10 min. The preferential exploration index was calculated as the ratio of the duration of contacts with the object in position #1 over the total duration of contacts



with both objects. For rats, 16 days after A $\beta$  injection, rats were placed individually in a squared open-field and two trials spaced by 2 h interval were performed. During the first trial (acquisition trial), rats were placed in the arena containing 2 identical objects and time required by each animal to complete 15 s of object exploration were determined. For the second trial (testing trial), one of the objects presented in the first trial was replaced by an unknown object (novel object). Rats were placed back in the arena and exploration of each object was determined. For both trials, locomotor activity of rats was scored. Only animals having a minimal level of object exploration of 5 s during the testing trial were included in the study. The time spent in active exploration of the novel object and the familiar object (Delta Novel-Familiar) was measured.

**Spontaneous alternation in the Y-maze**<sup>68</sup>. 7 days after A $\beta$ <sub>25–35</sub> or Sc.A $\beta$  peptide injection, each mouse was placed at the end of one arm in a grey polyvinylchloride Y-maze. The series of arm entries, including possible returns into the same arm, was recorded visually. An alternation was defined as entries into all three arms on consecutive occasions. The number of the maximum alternations was the total number of arm entries minus two and the percentage of alternation was calculated as actual alternations/maximum alternations  $\times$  100. Measured parameters included the percentage of alternation (memory index) and total number of arm entries (exploration index).

**Step through type passive avoidance**<sup>69</sup>. Briefly, the apparatus consisted of two compartments with one illuminated with white polyvinylchloride walls and the other darkened with black polyvinylchloride walls and a grid floor for electrical shocks. A guillotine door separated each compartment. 8 days after A $\beta$ <sub>25–35</sub> or Sc.A $\beta$  peptide injection, each mouse was placed into the white compartment. After 5 s, the door was raised. When the mouse entered the darkened compartment and placed all its paws on the grid floor, the door was closed and the foot shock (0.3 mA) delivered for 3 s. The latency spent to enter the dark compartment and the number of vocalisations were recorded. The number of vocalisations did not differ among groups, indicating that shock sensitivity was unaffected by the treatments (data not shown). The retention test was carried out 24 h after training (9 days after A $\beta$ <sub>25–35</sub> or Sc.A $\beta$  peptide injection). Each mouse was placed again into the white compartment. After 5 s, the door was raised and the step-through latency (latency to enter the dark compartment) was recorded up to 300 s.

**Histology**. Eight days after A $\beta$ <sub>25–35</sub> or Sc.A $\beta$  injection, each mouse was anaesthetised by intramuscular injection of 80 mg Kg<sup>-1</sup> ketamine and 10 mg Kg<sup>-1</sup> xylazine, and quickly perfused transcardially with 100 mL of saline solution followed by 100 mL of paraformaldehyde 4%. Brains were removed and kept for 24 h in the fixative solution at +4°C, then cut in coronal sections (20  $\mu$ m) using a vibratome (Leica VT1000 S, Wetzlar, Germany). Sections were stained with 0.2% cresyl violet reagent (Sigma), dehydrated with graded ethanol, treated with toluene and mounted with Mountex medium (BDH Laboratory Supplies, Poole, Dorset, UK). Examination of the CA1 area was performed using a light microscope (Dialux 22, Leitz, Wetzlar, Germany), slices being digitalised through a CCD camera (Sony XC-77CE, Sony, Paris, France) with the NIH Image version 1.63 software. CA1 measurement and pyramidal cell count have been processed by ImageJ (NIH). Data were calculated as average of 8 slices and expressed as number of CA1 pyramidal cells per millimetre for each group.

**Blood-brain barrier (BBB) permeability**. Seven days after A $\beta$ <sub>25–35</sub> or Sc.A $\beta$  peptide injection, Evans Blue (EB) dye (2% in saline, 4 mL Kg<sup>-1</sup>) was injected i.p. 3 h prior to the transcardiac perfusion. Mice were anaesthetised i.p. with 200  $\mu$ L of pre-mix 80 mg Kg<sup>-1</sup> ketamine and 10 mg Kg<sup>-1</sup> xylazine, then perfused transcardially with 250 mL of saline solution. After decapitation, the brain was removed, dissected and weighed for quantitative measurement of EB extravasation. Samples were homogenized in PBS and mixed by vortexing after the addition of 60% trichloroacetic acid to precipitate the protein. Samples were cooled at +4°C, and then centrifuged 30 min at 10,000 g at +4°C. The supernatant was measured at 610 nm for absorbance of EB using a spectrophotometer. EB quantification was expressed as pg per mg of brain tissue.

**Biochemical analyses**. Seven (synaptophysin), 8 (GFAP), or 9 (A $\beta$ <sub>1–42</sub>, cPARP, BDNF, IL-1 $\beta$ , TNF $\alpha$ ) days after A $\beta$ <sub>25–35</sub> or Sc.A $\beta$  injection, hippocampi were dissected out and rinsed in ice-cold PBS to remove excess blood, and weighed before nitrogen freezing and –80°C storage. Tissues were cut into small pieces, homogenised, sonicated and centrifuged. The supernatants were assayed immediately by ELISA for GFAP, synaptophysin, IL-1 $\beta$  (USCN, China), TNF $\alpha$  (Thermo Scientific, France), BDNF (Promega, France), cPARP (Cell Signalling, France) and A $\beta$ <sub>1–42</sub> (Euromedex, France) following manufacturer's recommendations. All samples were assayed in duplicate and only samples for which the CV was <25% between replicates were included for analyses. Results were expressed in pg protein per mg of brain tissue, or as % of Sc. control. Protein concentration was determined in brain homogenates with the BCA protein assay kit (Pierce Perbio Science, France).

**Lipid peroxidation**. Briefly, mice were killed by decapitation and hippocampi were rapidly isolated, weighed, and kept in liquid nitrogen until assayed. After thawing, brains were homogenised in cold methanol (1:10, w/v), centrifuged at 1,000 g during 5 min at room temperature and supernatants collected. Homogenate was added to a solution containing 1 mM FeSO<sub>4</sub>, 0.25 M H<sub>2</sub>SO<sub>4</sub>, 1 mM xylene orange, and incubated for 30 min at room temperature. Absorbance was measured at 580 nm (A<sub>580</sub>1), and 10  $\mu$ L of 1 mM cumene hydroperoxide (CHP) was added to the sample

and incubated for 30 min at room temperature to determine the maximal oxidation level. Absorbance was measured at 580 nm (A<sub>580</sub>2). The level of lipid peroxidation was determined as CHP equivalents according to: CHP equivalent = A<sub>580</sub>1/A<sub>580</sub>2  $\times$  (CHP (nmol))  $\times$  dilution, and expressed as CHP equivalents per mg tissue.

**Statistical analyses**. Statistical tests were two-tailed, and conducted at a 5% significance level. Sample sizes used for behavioural analyses were defined on the basis on previous experience on assay variability. Data distribution and within-group variation were preliminary assessed in order to guide our methodological choices. We applied an Analysis of Variance (ANOVA) with Dunnett's test for comparison of more than one experimental group against a reference. A *t*-test was also used as a supportive technique. For repeated measures data (MWM acquisition and working memory tests in Figures 2a,b,f,g) we applied a mixed ANOVA with Dunnett's test, including fixed effect terms for treatment, time and the treatment by time interaction, and a random effect term for animals. Treatment effect was assessed at each time point and for combined time points (global effect). Group comparisons were performed with Prism (<http://www.graphpad.com/scientific-software/prism>).

Drug combination analyses with calculation of Combination Indexes (CI) and isobolograms<sup>70</sup> were performed with R (<http://cran.r-project.org>). Briefly, CI compares dosages for a given combination to those expected to obtain the same combination effect under a simple additive assumption, and offers a quantitative definition for additive effect (CI = 1), synergism (CI < 1), and antagonism (CI > 1) in drug combinations. Isobologram is a popular graph introduced by Loewe<sup>71</sup> constructed for a given effect level on a coordinate system composed of the individual drug doses (Supplementary Fig. 1c). In particular, doses of drug A and drug B (each alone) that give this effect are plotted as axial points. The line connecting these points represents dose pairs that will produce this effect in a simply additive combination. This line of additivity allows a comparison with the actual dose pair that produces this effect level experimentally, and is employed to distinguish additive from synergistic (below the line) and antagonistic (over the line) combinations.

- Mullane, K. & Williams, M. Alzheimer's therapeutics: continued clinical failures question the validity of the amyloid hypothesis-but what lies beyond? *Biochem. Pharmacol.* **85**, 289–305 (2013).
- Potter, P. E. Investigational medications for treatment of patients with Alzheimer disease. *J. Am. Osteopath. Assoc.* **110**, S27–36 (2010).
- Querfurth, H. W. & LaFerla, F. M. Alzheimer's disease. *N. Engl. J. Med.* **362**, 329–44 (2010).
- Zlokovic, B. V. The blood-brain barrier in health and chronic neurodegenerative disorders. *Neuron* **57**, 178–201 (2008).
- Iadecola, C. The overlap between neurodegenerative and vascular factors in the pathogenesis of dementia. *Acta Neuropathol.* **120**, 287–96 (2010).
- Berk, C. & Sabbagh, M. N. Successes and failures for drugs in late-stage development for Alzheimer's disease. *Drugs Aging* **30**, 783–92 (2013).
- Pimentel-Coelho, P. M. & Rivest, S. The early contribution of cerebrovascular factors to the pathogenesis of Alzheimer's disease. *Eur. J. Neurosci.* **35**, 1917–37 (2012).
- Paula-Lima, A. C., Brito-Moreira, J. & Ferreira, S. T. Deregulation of excitatory neurotransmission underlying synapse failure in Alzheimer's disease. *J. Neurochem.* **126**, 191–202 (2013).
- Rissman, R. A. & Mobley, W. C. Implications for treatment: GABAA receptors in aging, Down syndrome and Alzheimer's disease. *J. Neurochem.* **117**, 613–22 (2011).
- Limon, A., Reyes-Ruiz, J. M. & Miledi, R. Loss of functional GABA(A) receptors in the Alzheimer diseased brain. *Proc. Natl. Acad. Sci. U. S. A.* **109**, 10071–6 (2012).
- Appleby, B. S. & Cummings, J. L. Discovering new treatments for Alzheimer's disease by repurposing approved medications. *Curr. Top. Med. Chem.* **13**, 2306–27 (2013).
- Dahchour, A. *et al.* Central effects of acamprosate: part 1. Acamprosate blocks the glutamate increase in the nucleus accumbens microdialysate in ethanol withdrawn rats. *Psychiatry Res.* **82**, 107–14 (1998).
- Willard, S. S. & Koochekpour, S. Glutamate, Glutamate Receptors, and Downstream Signaling Pathways. *Int. J. Biol. Sci.* **9**, 948–959 (2013).
- Revet, T. J., Baker, G. B., Jhamandas, J. & Kar, S. Glutamate system, amyloid  $\beta$  peptides and tau protein: functional interrelationships and relevance to Alzheimer disease pathology. *J. Psychiatry Neurosci.* **38**, 6–23 (2013).
- De Witte, P., Littleton, J., Parot, P. & Koob, G. Neuroprotective and abstinence-promoting effects of acamprosate: elucidating the mechanism of action. *CNS Drugs* **19**, 517–37 (2005).
- Chau, P., Stomberg, R., Fagerberg, A., Söderpalm, B. & Ericson, M. Glycine receptors involved in acamprosate's modulation of accumbal dopamine levels: an in vivo microdialysis study. *Alcohol. Clin. Exp. Res.* **34**, 32–8 (2010).
- Collard, C. D. *et al.* Neutrophil-derived glutamate regulates vascular endothelial barrier function. *J. Biol. Chem.* **277**, 14801–11 (2002).
- Van Den Eynden, J. *et al.* Glycine and glycine receptor signalling in non-neuronal cells. *Front. Mol. Neurosci.* **2**, 9 (2009).
- Shastry, S. *et al.* GABA receptors ameliorate Hcy-mediated integrin shedding and constrictive collagen remodeling in microvascular endothelial cells. *Cell Biochem. Biophys.* **45**, 157–65 (2006).
- LaFerla, F. M. & Green, K. N. Animal models of Alzheimer disease. *Cold Spring Harb. Perspect. Med.* **2**, a006320 (2012).





21. Callizot, N., Combes, M., Steinschneider, R. & Poindron, P. Operational dissection of  $\beta$ -amyloid cytopathic effects on cultured neurons. *J. Neurosci. Res.* **91**, 706–16 (2013).
22. Hayashi, S. *et al.* Alzheimer disease-associated peptide, amyloid beta40, inhibits vascular regeneration with induction of endothelial autophagy. *Arterioscler. Thromb. Vasc. Biol.* **29**, 1909–15 (2009).
23. Eckert, G. P. *et al.* Mitochondrial dysfunction—a pharmacological target in Alzheimer's disease. *Mol. Neurobiol.* **46**, 136–50 (2012).
24. Pohanka, M. Alzheimer's disease and oxidative stress: a review. *Curr. Med. Chem.* **21**, 356–64 (2013).
25. Esposito, Z. *et al.* Amyloid  $\beta$ , glutamate, excitotoxicity in Alzheimer's disease: are we on the right track? *CNS Neurosci. Ther.* **19**, 549–55 (2013).
26. Avila, J. Tau phosphorylation and aggregation in Alzheimer's disease pathology. *FEBS Lett.* **580**, 2922–7 (2006).
27. Amadoro, G. *et al.* Interaction between NH(2)-tau fragment and A $\beta$  in Alzheimer's disease mitochondria contributes to the synaptic deterioration. *Neurobiol. Aging* **33**, 833.e1–25 (2012).
28. Chambon, C., Wegener, N., Gravius, A. & Danysz, W. Behavioural and cellular effects of exogenous amyloid- $\beta$  peptides in rodents. *Behav. Brain Res.* **225**, 623–41 (2011).
29. Zussy, C. *et al.* Time-course and regional analyses of the physiopathological changes induced after cerebral injection of an amyloid  $\beta$  fragment in rats. *Am. J. Pathol.* **179**, 315–34 (2011).
30. Zussy, C. *et al.* Alzheimer's disease related markers, cellular toxicity and behavioral deficits induced six weeks after oligomeric amyloid- $\beta$  peptide injection in rats. *PLoS One* **8**, e53117 (2013).
31. Balducci, C. & Forloni, G. In Vivo Application of Beta Amyloid Oligomers: a Simple Tool to Evaluate Mechanisms of Action and New Therapeutic Approaches. *Curr. Pharm. Des.* **20**, 2491–505 (2013).
32. Kaminsky, Y. G., Marlatt, M. W., Smith, M. A. & Kosenko, E. A. Subcellular and metabolic examination of amyloid-beta peptides in Alzheimer disease pathogenesis: evidence for A $\beta$ (25–35). *Exp. Neurol.* **221**, 26–37 (2010).
33. Logue, S. F., Paylor, R. & Wehner, J. M. Hippocampal lesions cause learning deficits in inbred mice in the Morris water maze and conditioned-fear task. *Behav. Neurosci.* **111**, 104–13 (1997).
34. Antunes, M. & Biala, G. The novel object recognition memory: neurobiology, test procedure, and its modifications. *Cogn. Process.* **13**, 93–110 (2012).
35. Lalonde, R. The neurobiological basis of spontaneous alternation. *Neurosci. Biobehav. Rev.* **26**, 91–104 (2002).
36. Rudy, J. W., Huff, N. C. & Matus-Amat, P. Understanding contextual fear conditioning: insights from a two-process model. *Neurosci. Biobehav. Rev.* **28**, 675–85 (2004).
37. Marchetti, C. & Marie, H. Hippocampal synaptic plasticity in Alzheimer's disease: what have we learned so far from transgenic models? *Rev. Neurosci.* **22**, 373–402 (2011).
38. Cai, Z., Zhao, B. & Ratka, A. Oxidative stress and  $\beta$ -amyloid protein in Alzheimer's disease. *Neuromolecular Med.* **13**, 223–50 (2011).
39. Strosznajder, J. B., Czapski, G. a., Adamczyk, A. & Strosznajder, R. P. Poly(ADP-ribose) polymerase-1 in amyloid beta toxicity and Alzheimer's disease. *Mol. Neurobiol.* **46**, 78–84 (2012).
40. Heneka, M. T., O'Banion, M. K., Terwel, D. & Kummer, M. P. Neuroinflammatory processes in Alzheimer's disease. *J. Neural Transm.* **117**, 919–47 (2010).
41. Verkhratsky, A., Olabarria, M., Noristani, H. N., Yeh, C.-Y. & Rodriguez, J. J. Astrocytes in Alzheimer's disease. *Neurotherapeutics* **7**, 399–412 (2010).
42. Palop, J. J. & Mucke, L. Amyloid-beta-induced neuronal dysfunction in Alzheimer's disease: from synapses toward neural networks. *Nat. Neurosci.* **13**, 812–8 (2010).
43. Meunier, J., Villard, V., Givalois, L. & Maurice, T. The  $\gamma$ -secretase inhibitor 2-[(1R)-1-[(4-chlorophenyl)sulfonyl]](2,5-difluorophenyl) amino]ethyl-5-fluorobenzenecarboxylic acid (BMS-299897) alleviates A $\beta$ 1–42 seeding and short-term memory deficits in the A $\beta$ 25–35 mouse model of Alzheimer's disease. *Eur. J. Pharmacol.* **698**, 193–9 (2013).
44. Kimura, N., Takahashi, M., Tashiro, T. & Terao, K. Amyloid beta up-regulates brain-derived neurotrophic factor production from astrocytes: rescue from amyloid beta-related neuritic degeneration. *J. Neurosci. Res.* **84**, 782–9 (2006).
45. Frautschy, S. A. & Cole, G. M. Why pleiotropic interventions are needed for Alzheimer's disease. *Mol. Neurobiol.* **41**, 392–409 (2010).
46. Ainsworth, C. Networking for new drugs. *Nat. Med.* **17**, 1166–8 (2011).
47. Ulrich, D. & Bettler, B. GABA(B) receptors: synaptic functions and mechanisms of diversity. *Curr. Opin. Neurobiol.* **17**, 298–303 (2007).
48. Tu, H. *et al.* GABAB receptor activation protects neurons from apoptosis via IGF-1 receptor transactivation. *J. Neurosci.* **30**, 749–59 (2010).
49. Sharp, C. D. *et al.* Glutamate causes a loss in human cerebral endothelial barrier integrity through activation of NMDA receptor. *Am. J. Physiol. Heart Circ. Physiol.* **285**, H2592–8 (2003).
50. Gillard, S. E., Tzafaris, J., Tsui, H.-C. T. & Kingston, A. E. Expression of metabotropic glutamate receptors in rat meningeal and brain microvasculature and choroid plexus. *J. Comp. Neurol.* **461**, 317–32 (2003).
51. Mason, B. J. Treatment of alcohol-dependent outpatients with acamprosate: a clinical review. *J. Clin. Psychiatry* **62 Suppl 2**, 42–8 (2001).
52. Spanagel, R. *et al.* Acamprosate produces its anti-relapse effects via calcium. *Neuropsychopharmacology* **39**, 783–91 (2014).
53. Rammes, G. *et al.* The anti-craving compound acamprosate acts as a weak NMDA-receptor antagonist, but modulates NMDA-receptor subunit expression similar to memantine and MK-801. *Neuropharmacology* **40**, 749–60 (2001).
54. Popp, R. L. & Lovinger, D. M. Interaction of acamprosate with ethanol and spermine on NMDA receptors in primary cultured neurons. *Eur. J. Pharmacol.* **394**, 221–31 (2000).
55. Harris, B. R. *et al.* Acamprosate inhibits the binding and neurotoxic effects of trans-ACPD, suggesting a novel site of action at metabotropic glutamate receptors. *Alcohol. Clin. Exp. Res.* **26**, 1779–93 (2002).
56. Lee, H. *et al.* Aberrant expression of metabotropic glutamate receptor 2 in the vulnerable neurons of Alzheimer's disease. *Acta Neuropathol.* **107**, 365–71 (2004).
57. Caraci, F. *et al.* Targeting group II metabotropic glutamate (mGlu) receptors for the treatment of psychosis associated with Alzheimer's disease: selective activation of mGlu2 receptors amplifies beta-amyloid toxicity in cultured neurons, whereas dual activation of mGlu2 an. *Mol. Pharmacol.* **79**, 618–26 (2011).
58. Um, J. W. *et al.* Metabotropic glutamate receptor 5 is a coreceptor for Alzheimer a $\beta$  oligomer bound to cellular prion protein. *Neuron* **79**, 887–902 (2013).
59. Hamilton, A., Esseltine, J. L., DeVries, R. a., Cregan, S. P. & Ferguson, S. S. G. Metabotropic glutamate receptor 5 knockout reduces cognitive impairment and pathogenesis in a mouse model of Alzheimer's disease. *Mol. Brain* **7**, 40 (2014).
60. Westmark, C. J. & Malter, J. S. FMRP mediates mGluR5-dependent translation of amyloid precursor protein. *PLoS Biol.* **5**, e52 (2007).
61. Kim, S. H. *et al.* Group II metabotropic glutamate receptor stimulation triggers production and release of Alzheimer's amyloid(beta)42 from isolated intact nerve terminals. *J. Neurosci.* **30**, 3870–5 (2010).
62. Danglot, L., Rostaing, P., Triller, A. & Bessis, A. Morphologically identified glycinergic synapses in the hippocampus. *Mol. Cell. Neurosci.* **27**, 394–403 (2004).
63. Ryu, J. K. & McLarnon, J. G. A leaky blood-brain barrier, fibrinogen infiltration and microglial reactivity in inflamed Alzheimer's disease brain. *J. Cell. Mol. Med.* **13**, 2911–25 (2009).
64. Zahs, K. R. & Ashe, K. H. “Too much good news” - are Alzheimer mouse models trying to tell us how to prevent, not cure, Alzheimer's disease? *Trends Neurosci.* **33**, 381–9 (2010).
65. Havas, D. *et al.* A longitudinal study of behavioral deficits in an A $\beta$ PP transgenic mouse model of Alzheimer's disease. *J. Alzheimers. Dis.* **25**, 231–43 (2011).
66. Necula, M., Kaye, R., Milton, S. & Glabe, C. G. Small molecule inhibitors of aggregation indicate that amyloid beta oligomerization and fibrillization pathways are independent and distinct. *J. Biol. Chem.* **282**, 10311–24 (2007).
67. Morris, R. G. Spatial Localization Does Not Require the Presence of Local Cues. *Learn. Motiv.* **12**, 239–260 (1981).
68. Maurice, T., Lockhart, B. P. & Privat, A. Amnesia induced in mice by centrally administered beta-amyloid peptides involves cholinergic dysfunction. *Brain Res.* **706**, 181–93 (1996).
69. Villard, V. *et al.* Antiamnesic and neuroprotective effects of the aminotetrahydrofuran derivative ANAVEX1-41 against amyloid beta(25–35)-induced toxicity in mice. *Neuropsychopharmacology* **34**, 1552–66 (2009).
70. Tallarida, R. J. An overview of drug combination analysis with isobolograms. *J. Pharmacol. Exp. Ther.* **319**, 1–7 (2006).
71. Loewe, S. The problem of synergism and antagonism of combined drugs. *Arzneimittelforschung* **3**, 285–90 (1953).

## Acknowledgments

We would like to thank Dr Birgit Hutter-Paier for her technical assistance with regard to transgenic models. We are also grateful to Ms Linda Belo for reviewing the English of the manuscript. This work was funded by Pharnext.

## Author contributions

D.C. generated the strategic vision of the project. I.C., S.N. and D.C. contributed to the overall study design. I.C. and S.N. participated in target Network definition, S.N. proposed candidate molecules for screening, Y.P. and E.G. contributed to selection of candidate molecules for screening. I.C., R.H. and E.V. supervised the experimental part *in vitro* and *in vivo*. R.H., N.Ch., A.M., A.B. and D.T. designed and analysed the experiments. N.Ca. and R.S. advised and participated in the analyses of the *in vitro* part of the project, while T.M. advised and participated in the analyses of the *in vivo* part. M.G., J.F. and S.T. performed the combined analyses of *in vitro* and *in vivo* experiments and advised on statistical designs. C.S.G. and V.B. advised for the clinically relevant endpoints in animal models. R.H. organised the data, provided the major input in their presentation and drafted the first version of the manuscript. R.H. and I.C. were responsible for the writing and editing of the manuscript. S.N. and D.C. also contributed in writing the manuscript. All authors reviewed and approved the manuscript.

## Additional information

Supplementary information accompanies this paper at <http://www.nature.com/scientificreports>

**Competing financial interests:** A.B., A.M., C.S.G., D.C., E.G., I.C., J.F., M.G., N.Ch., R.H., S.N., S.T., V.B. and Y.P. are present employees of Pharnext. E.V. and S.T. are former employee of Pharnext. D.C., E.V., I.C., M.G., N.Ch., S.N., E.G., R.H. and V.B. are designated on patent applications held by Pharnext. R.S. is the CEO of Neuronexperts and N.Ca. is



presently at Neuro/Sys. T.M. is the CSO of Amylgen and research director in a public institution (INSERM U710).

**How to cite this article:** Chumakov, I. *et al.* Combining two repurposed drugs as a promising approach for Alzheimer's disease therapy. *Sci. Rep.* 5, 7608; DOI:10.1038/srep07608 (2015).



This work is licensed under a Creative Commons Attribution 4.0 International License. The images or other third party material in this article are included in the article's Creative Commons license, unless indicated otherwise in the credit line; if the material is not included under the Creative Commons license, users will need to obtain permission from the license holder in order to reproduce the material. To view a copy of this license, visit <http://creativecommons.org/licenses/by/4.0/>